lubricants

MDPI

Article

A BPNN-QSTR Model for Friction-Reducing Performance of Organic Liquid Lubricants on SiC/PI Friction Pair

Tingting Wang [1], Liang Zhang [1], Hao Chen [1], Li Wu [2] and Xinlei Gao [3,*]

[1] School of Chemical and Environmental Engineering, Wuhan Polytechnic University, Wuhan 430023, China; tt_wang88@163.com (T.W.)
[2] School of Chemistry and Environmental Engineering, Wuhan Institute of Technology, Wuhan 430074, China
[3] School of Materials Science and Engineering, Hubei University, Wuhan 430062, China
* Correspondence: gaoxl0131@163.com

Abstract: In this study, a systematic test of 36 organic liquid compounds as lubricants in the SiC/PI friction pair was conducted to investigate their friction-reducing performance. The back propagation neural network (BPNN) method was employed to establish a quantitative structure tribo-ability relationship (QSTR) model for the friction performance of these lubricants. The developed BPNN-QSTR model exhibited excellent fitting and predictive accuracy, with R^2 = 0.9700, R^2 (*LOO*) = 0.6570, and q^2 = 0.8606. The impact of different descriptors in the model on the friction-reducing performance of the lubricants was explored. The results provide valuable guidance for the design and optimization of lubricants in SiC/PI friction systems, contributing to the development of high-performance lubrication systems.

Keywords: organic liquid lubricants; quantitative structure tribo-ability relationship; back propagation neural network; friction-reducing performance

Citation: Wang, T.; Zhang, L.; Chen, H.; Wu, L.; Gao, X. A BPNN-QSTR Model for Friction-Reducing Performance of Organic Liquid Lubricants on SiC/PI Friction Pair. *Lubricants* **2023**, *11*, 387. https://doi.org/10.3390/lubricants11090387

Received: 31 July 2023
Revised: 27 August 2023
Accepted: 8 September 2023
Published: 10 September 2023

1. Introduction

Currently, the Earth is facing numerous serious environmental issues. Against the backdrop of global climate change, the "low-carbon economy" based on low energy consumption and low pollution has become a global hotspot. Adopting new concepts, technologies, and methods in the industrial sector to improve energy efficiency, develop emerging industries, and reduce energy consumption is an inevitable choice for achieving win-win economic development and resource and environmental protection. The research on tribology has continuously made significant contributions to meeting the needs of these advanced technological developments [1]. Friction is one of the important pathways for energy loss, and reducing friction can effectively improve production efficiency, reduce energy consumption, and is an important aspect of achieving a low-carbon economy and sustainable social development. In recent years, due to its ability to significantly improve the energy utilization efficiency of motion systems, the study of superlubricity has become a research hotspot in the field of friction [2]. In macroscopic systems, the phenomenon of ultra-low friction with friction coefficients on the order of 0.001 or below is generally referred to as superlubrication. Since the concept was proposed in the 1990s [3], extensive research has been conducted on the superlubricity of solids and liquids over the past three decades [4–7].

The design and development of novel lubrication systems are effective means to achieve superlubricity. One important element of a lubrication system is the friction pair material. Polyimide is a type of high-performance engineering plastic material, typically synthesized from diamines and dianhydrides. Its molecular chain contains imide bonds and stable aromatic heterocyclic structures, which give it excellent mechanical properties, radiation resistance, self-lubricating properties, and processability [8]. As a result, research

and applications of polyimide in the field of friction are gradually expanding [9–13]. Ceramic materials also possess high hardness, strength, stiffness, low density, and excellent chemical stability. Their excellent mechanical properties at high temperatures make them widely used in space technology, sealing components, critical engine parts, high-efficiency high-speed cutting tools, and other fields, making them one of the best choices for high-temperature wear-resistant materials [14]. In recent years, researchers have conducted studies on friction systems composed of SiC ceramics as friction components paired with different materials such as metals, composite materials, and SiC itself [15–19]. However, there have been no reports on the SiC/PI friction pair system to date. Due to the excellent frictional properties of both materials, it can be anticipated that exploring a high-performance lubrication system using SiC and PI as a pair would be a feasible approach.

Due to the strict requirement for atomic-level smooth contact on material surfaces, frictional systems under dry sliding conditions at the macroscopic scale rarely achieve solid superlubricity. In comparison, many lubrication systems incorporating liquid media (such as water, alcohols, acids, ionic liquids, etc.) exhibit macroscopic superlubricity [6]. The prospects of the liquid superlubricity in industrial applications are excellent. Based on the demand for environmentally friendly industrial applications, this study focuses on high-performance, low-cost, environmentally friendly organic liquid compounds as the target, to explore the tribological performance of SiC/PI friction pairs lubricated with such lubricants.

The development of novel lubricants in the past required extensive experimental work to synthesize compounds, followed by tribological performance testing, and further screening and optimization of molecular structures. This entire process lacked clear theoretical guidance and was prone to some degree of trial and error. By using Quantitative Structure Tribo-ability Relationship (QSTR) theory to predict the tribological performance of compounds, it is possible to effectively avoid large-scale repetitive experimental work and achieve efficient and low-energy design or selection of lubricants. QSTR is a concept derived and developed from Quantitative Structure-Activity Relationship (QSAR) methods widely used in fields such as pharmacology. QSAR is an effective method for quantitative calculation or approximate estimation, which establishes mathematical relationships between the physicochemical properties and physical and chemical activities (descriptors) of a class of compounds. Based on the foundation of QSAR theory, our research team has attempted to view the tribological performance of lubricating media as complex physicochemical properties of compounds. We have developed the concept of QSTR and conducted extensive work. QSTR models were established for the tribological performance of lubricating oils and lubricant additives, respectively. The results have confirmed the feasibility of the QSTR method in studying the relationship between the structure and tribological ability of materials. Additionally, the analysis of these models allows us to further understand the relationship between material structural characteristics and tribological features. Based on these models, we have successfully conducted molecular design of new lubricants [20–22]. Based on our previous research findings, the BPNN-QSTR models have shown excellent performance in predicting the tribological properties of lubricants. As an important nonlinear modeling method, back propagation neural network (BPNN) plays a crucial role in quantitative structure-activity relationship studies. The field of tribology encompasses intricate frictional phenomena and interactions, often involving nonlinear factors. Consequently, when compared to linear methods, the BPNN approach exhibits superior adaptability and explanatory power in relation to these complex frictional phenomena, thereby providing more precise and comprehensive prediction outcomes.

This article aims to investigate the correlation between the friction-reducing performance and molecular structure of organic liquid lubricants on the SiC/PI friction pair based on the theory of QSTR. By establishing a quantitative model using BPNN method, the friction-reducing performance of these lubricants in the system will be predicted, and the mechanisms of friction reduction will be explored. Furthermore, guidance and recommendations will be provided for the synthesis or modification of lubricant molecules with

good friction-reducing performance. As this is our first time establishing a BPNN-QSTR model for the lubricant medium in SiC/PI system, we will choose a selection of compounds from different categories with relatively simple structures to conduct this work. This choice will allow us to accurately understand the influence of lubricant structural factors.

2. Materials and Methods

2.1. Experimental Materials

In this study, 36 different types of common organic compounds, including alcohols, alkanes, and esters, were selected as lubricants for frictional testing. All reagents were purchased from Aladdin Reagent Company, Shanghai, China and remained stable in a liquid state under normal temperature and pressure conditions. The specific molecular names and chemical formulas can be found in Table 1. The friction pair materials consisted of SiC ceramic balls (with a diameter of 4.76 mm) produced by Fanlian Technology Co., Ltd., Shanghai, China, and a polyimide film composed of pyromellitic dianhydride (PMDA) and 4,4′-oxydianiline (ODA) produced by DuPont Company, Wilmington, DE, USA(with a thickness of 127 μm). The structure of the polyimide (PI) is shown in Figure 1.

Table 1. Experimental and predicted data of lubricants.

No.	Name	Formula	*COF*	MF_{expt}	MF_{pred}	Δ
1	ethane-1,2-diol	$C_2H_6O_2$	0.06891	1.502	1.498	−0.004
2 *	butane-1,4-diol	$C_4H_{10}O_2$	0.00391	1.353	1.499	0.146
3	propane-1,2,3-triol	$C_3H_8O_3$	0.00461	1.380	1.378	−0.002
4	6-chlorohexan-1-ol	$C_6H_{13}ClO$	0.01082	1.642	1.678	0.036
5	octan-1-ol	$C_8H_{18}O$	0.05532	1.800	1.744	−0.056
6	2-ethylhexan-1-ol	$C_8H_{18}O$	0.05811	1.805	1.785	−0.020
7	octan-2-ol	$C_8H_{18}O$	0.05267	1.795	1.808	0.013
8 *	nonan-1-ol	$C_9H_{20}O$	0.01969	1.732	1.693	−0.039
9	2-(benzylamino)ethanol	$C_9H_{13}NO$	0.01860	1.747	1.742	−0.005
10	decan-1-ol	$C_{10}H_{22}O$	0.00239	1.544	1.661	0.117
11	undecan-1-ol	$C_{11}H_{24}O$	0.01486	1.779	1.693	−0.086
12	octanoic acid	$C_8H_{16}O_2$	0.03073	1.781	1.777	−0.004
13	(Z)-octadec-9-enoic acid	$C_{18}H_{34}O_2$	0.02924	2.067	2.071	0.004
14 *	nonanal	$C_9H_{18}O$	0.02535	1.754	1.705	−0.049
15	decanal	$C_{10}H_{20}O$	0.01193	1.713	1.712	−0.001
16	1-(4-methylphenyl)propan-1-one	$C_{10}H_{12}O$	0.02911	1.787	1.763	−0.024
17	methylsulfinylmethane	C_2H_6SO	0.04652	1.559	1.555	−0.004
18	2-chloro-1,3-benzoxazole	C_7H_4ClNO	0.02501	1.784	1.783	−0.001
19	1-bromooctane	$C_8H_{17}Br$	0.04780	1.953	1.943	−0.010
20	1-chlorodecane	$C_{10}H_{21}Cl$	0.04655	1.913	1.925	0.012
21 *	1-bromodecane	$C_{10}H_{21}Br$	0.05172	2.021	2.025	0.004
22	1-iododecane	$C_{10}H_{21}I$	0.03699	2.070	2.054	−0.016
23	1-bromododecane	$C_{12}H_{25}Br$	0.03017	2.015	2.019	0.004
24	1-chlorotetradecane	$C_{14}H_{29}Cl$	0.04010	2.017	1.994	−0.023
25 *	1-bromotetradecane	$C_{14}H_{29}Br$	0.01808	2.005	1.969	−0.036
26	hexadecane	$C_{16}H_{34}$	0.05724	2.044	2.060	0.016
27	1-bromohexadecane	$C_{16}H_{33}Br$	0.00716	1.947	1.942	−0.005
28	methyl 2-phenylacetate	$C_9H_{10}O_2$	0.01423	1.715	1.706	−0.009
29	methyl decanoate	$C_{11}H_{22}O_2$	0.04978	1.944	1.939	−0.005
30 *	methyl dodecanoate	$C_{13}H_{26}O_2$	0.03207	1.957	2.084	0.127
31	dimethyl propanedioate	$C_5H_8O_4$	0.02299	1.711	1.716	0.005
32	tert-butyl (2-methylpropan-2-yl)oxycarbonyl carbonate	$C_{10}H_{18}O_5$	0.01156	1.854	1.867	0.013
33 *	dibutyl butanedioate	$C_{12}H_{22}O_4$	0.00850	1.844	1.893	0.049
34	dibutyl benzene-1,2-dicarboxylate	$C_{16}H_{22}O_4$	0.00793	1.919	1.918	−0.001
35	triphenyl phosphite	$C_{18}H_{15}O_3P$	0.06006	2.186	2.171	−0.015
36	tris(2-methylphenyl) phosphate	$C_{21}H_{21}O_4P$	0.01231	2.089	2.099	0.010

* Test set.

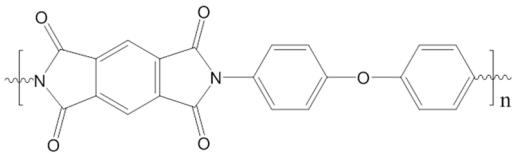

Figure 1. Molecular structure of polyimide.

2.2. Tribological Test

The tribological tests of the 36 organic compounds as lubricants was conducted using the rotating module of a multi-functional tribometer (UMT-3, CETR, CA, USA). The SiC ceramic ball and the PI (PMDA-ODA) film formed the friction pair. Prior to testing, the SiC ceramic ball, polyimide film and tribometer accessories were placed in petroleum ether, ultrasonically cleaned for 5 min, and then dried. The SiC ceramic ball was fixed on a steel holder as the stationary specimen (upper specimen), while the polyimide film was adhered to a smooth metal disc. The metal disc was then mounted on the fixed steel disc of the tribometer as the rotating specimen (lower specimen). Liquid lubricant was dropped onto the surface of the polyimide film to initiate the test. The applied load during the test was 5 N, the rotation speed was 250 rpm, the radius of rotation was 8.5 mm, and the test duration was 1 h. The tests were conducted at room temperature (25 °C) with a point-to-plane contact configuration. The coefficient of friction (COF) obtained during the test was automatically recorded and the average COF within 1 h was generated by the computer. The experimental data obtained are listed in Table 1.

2.3. Quantitative Structure Tribo-Ability Relationship Model

2.3.1. Experimental Data Processing

According to Formula (1), the experimental friction coefficient obtained from the tests on the lubricant are subjected to simple mathematical processing. This processing converts the data into a standardized quantity called the friction coefficient measurement (MF), as shown in Table 1. The MF value is used to characterize the friction-reducing performance of the lubricant and is employed for subsequent modeling analysis.

$$MF_{expt} = \log_{10}[COF^{1/4} \times MW] \quad (1)$$

In the formula, MF_{expt} represents the friction coefficient measurement for the organic lubricants, while *COF* and *MW*, respectively, denote the coefficient of friction and the molecular weight of the organic lubricants. It is evident that a smaller value of MF indicates better friction-reducing properties of the lubricant.

Randomly selecting 29 molecules (approximately 4/5 of the entire sample) from the sample population, they were assigned as the training set to adjust the model parameters and establish the QSTR model. The remaining 7 molecules (approximately 1/5 of the entire sample) were designated as the test set to evaluate the predictive capability of the model. During the grouping process, it was also important to ensure a relatively uniform distribution of the test set data within the entire dataset, avoiding the accidental bias in evaluation results caused by concentration or imbalanced distribution. The selected molecules for the test set in this study are indicated in Table 1, covering four categories: alcohols, aldehydes, alkanes, and esters. The MF values of the test set range from 1.353 to 2.021, which is within the distribution range of the entire dataset (1.353 to 2.186). Therefore, the selection of the test set is reasonable.

2.3.2. Modeling Method

In this study, an artificial neural network model was established using the backpropagation learning algorithm. Artificial neural networks are nonlinear processing techniques that simulate the structure and functionality of the human brain. Due to their strong adaptive capabilities, they have become an important method for quantitative structure-activity

relationship (QSAR) studies. The error backpropagation (BP) algorithm is commonly employed to establish the network model [23]. One advantage of this technique is its ability to construct complex models based on a large amount of data. During the training process, the network automatically disregards descriptors that do not contribute to the dependent attributes.

The BPNN-QSTR model was established following the four steps outlined below: Firstly, the molecular structures of all 36 sample molecules were generated using ChemBioOffice 2008. Secondly, the generated structures were subjected to energy minimization and database file generation using Tripos Sysbyl-X 1.1. Thirdly, molecular structure descriptors, including lipophilicity parameters, 2D topological parameters, and 3D Jurs parameters, were calculated using Discovery Studio 2.5 software. Finally, the training dataset was used to fit a BPNN model, with the structure descriptors as input layer variables and the friction coefficient measurement as the output layer variable. Suitable descriptors were selected to obtain the QSTR model. A detailed process is outlined in Figure 2.

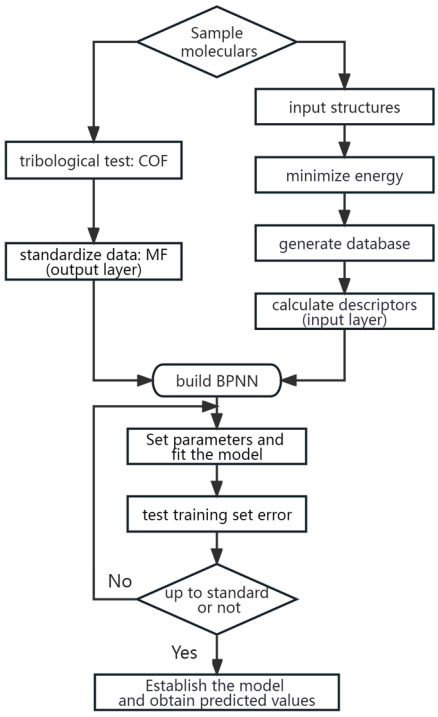

Figure 2. The Process of establishing the BPNN-QSTR Model.

In BPNN modeling, the number of nodes in the hidden layer is a crucial parameter that significantly impacts the performance of the BPNN model. Insufficient nodes in the hidden layer can lead to inadequate fitting accuracy, resulting in underfitting. Conversely, an excessive number of nodes may cause overfitting [24]. The fundamental principle for determining the number of hidden layer nodes is to select as few nodes as possible while meeting the accuracy requirements of the problem. Through multiple rounds of optimization training, the final number of nodes in the hidden layer is determined. The Leave One Out (LOO) method is employed for cross-validation during training.

3. Results and Discussion

3.1. Result of the Model

After multiple rounds of training and optimization, the optimal network structure obtained by the training set is 11-5-1. It means that there are 11 input variables (structural descriptors), 5 nodes in the hidden layer, and 1 output variable (MF). The fitting results of the obtained model are listed in Table 2, while the predicted values MF_{pred} and prediction

deviations Δ for the friction coefficient measurement are simultaneously presented in Table 1.

Table 2. Results of BPNN-QSTR model.

Network	R^2	R^2 (*LOO*)	q^2
11-5-1	0.9700	0.6570	0.8606

3.2. Validation of the Model

3.2.1. Internal Predictive Ability

The evaluation of the internal predictive ability of the BPNN model primarily focuses on the degree of fitting and prediction accuracy, as reflected by the correlation coefficient R^2 and the Leave-One-Out cross-validated correlation coefficient R^2 (*LOO*) in Table 2. These two fitting indices can measure the degree of fitting of the model to the training set, with values closer to 1 indicating a better fit to the data. From the results, the model demonstrates good accuracy ($R^2 > 0.9$, R^2 (*LOO*) > 0.6).

3.2.2. External Predictive Ability

The external predictive ability refers to the capability of using the established model to predict new compounds that were not used in the model training. This is a crucial indicator for evaluating the generalization ability and reliability of the model. Table 2 presents the correlation coefficient q^2 of the test set, calculated by Formula (2). This coefficient represents the error metric of the model and can be used to assess the external predictive ability.

$$q^2 = 1 - \frac{\sum_i (pred_i - \exp t_i)^2}{\sum_i (\exp t_i - \overline{\exp t})^2} \quad (2)$$

In the equation, $pred_i$ represents the predicted values of the test set, $expt_i$ represents the experimental values of the test set, and $\overline{expt}$ represents the average value of the experimental values in the test set. Typically, when $q^2 > 0.5$, the model is considered to have reliable predictive ability [25]. In this study, the calculated result for q^2 is 0.8606, which demonstrates a good external predictive ability.

3.2.3. Comparison of Predicted and Observed Values

Figure 3 displays the correlation between the calculated predicted results and the actual observed values for the entire dataset, providing a more intuitive representation of the model's strong predictive capability.

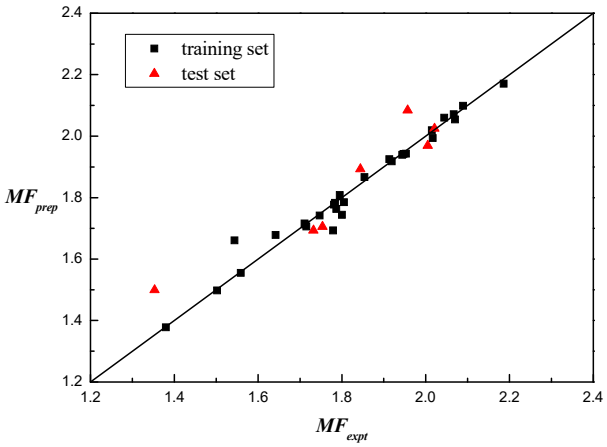

Figure 3. Prediction performance of the friction coefficient measurement.

3.3. Sensitivity Analysis on Descriptors

The sensitivity of descriptors in the BPNN model refers to the extent to which descriptors influence the output results of the model. Conducting sensitivity analysis on descriptors is of significant importance in optimizing the model, interpreting its prediction results, and guiding feature selection. It can enhance the predictive ability and interpretability of the BPNN model while also aiding in the optimization of data collection and feature selection processes. The input layer of the aforementioned BPNN model consists of 11 structural descriptors, which describe relevant molecular structural information as presented in Table 3. Figure 4 illustrates the magnitudes of sensitivity coefficients for each structural descriptor, which can be utilized to evaluate their relative contributions to the BPNN model. Larger absolute values of sensitivity coefficients indicate a greater impact of the descriptor on the model's output, while the positive or negative sign of the sensitivity coefficient represents its positive or negative influence on the model's predictive ability.

Table 3. Descriptors for the friction-reducing performance.

Descriptor	Description
ALogP	Log of the octanol-water partition coefficient using the atom-based method.
ES_Count_sOH	Calculate the E-state count for OH with one single bond.
Molecular_Weight	The sum of the atomic masses.
HBD_Count	Number of hydrogen bond donating groups in the molecule.
Num_H_Donors_Lipinski	Number of Hydrogen Bond Donors which are defined as heteroatoms (N, O, P, and S) with one or more attached Hydrogen atoms.
Molecular_PolarSASA	the sum of the solvent accessible surface area of all the selected polar elements, which can include N, O, P, and S.
Jurs_DPSA_2	Total charge weighted positive solvent-accessible surface area minus total charge weighted negative solvent-accessible surface area.
Jurs_DPSA_3	Atomic charge weighted positive solvent-accessible surface area minus atomic charge weighted negative solvent-accessible surface area.
Jurs_RNCG	Charge of most negative atom divided by the total negative charge.
Jurs_TASA	Sum of solvent-accessible surface areas of atoms with absolute value of partial charges less than 0.2.
Jurs_WNSA_2	Partial negative solvent-accessible surface area multiplied by the total negative charge, then multiplied by the total molecular solvent-accessible surface area and divided by 1000.

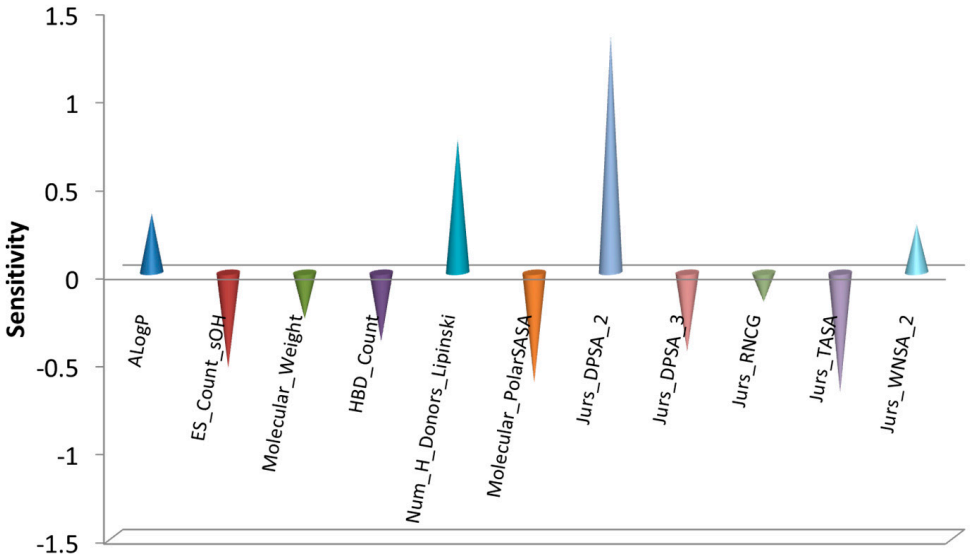

Figure 4. BPNN sensitivities of descriptors for the friction-reducing Performance.

3.3.1. Jurs Descriptors

Jurs descriptors are a type of three-dimensional molecular feature descriptor that combine shape and electronic information. They are calculated by mapping the partial charges of atoms onto individual atom-accessible surfaces [26]. These descriptors can be used to predict molecular polarity, solubility, adsorption properties, and more. The sensitivity results in Figure 3 indicate that Jurs descriptors play an important role in the model. A total of five Jurs descriptors were introduced in the model, suggesting that the polarity interaction between the lubricant molecules of this type and the SiC/PI friction pair surface plays a crucial role in their friction-reducing performance.

These five descriptors exhibit varying sensitivities and positive/negative influences in the model. Each descriptor reflects the molecular shape and charge distribution information from different perspectives, revealing the tendencies and differences of different types of atoms or functional groups in polar interactions. Specifically, Jurs_DPSA_2 and Jurs_DPSA_3 consider the charge states of the entire molecule and each individual atom, providing information about the polarity and solvent interactions of the entire molecule and different atoms within the molecule. Jurs_TASA only calculates atoms with lower electronegativity, while Jurs_WNSA_2 and Jurs_RNCG target negatively charged atoms. These descriptors yield abstract numerical values through complex calculations, making it difficult to provide a structural interpretation intuitively. However, the friction-reducing performance exhibited by lubricants is ultimately the result of the combined influence of these multiple factors. Therefore, by directly calculating these quantified values and utilizing the BPNN model, we can effectively predict the friction-reducing performance of the target molecule.

3.3.2. Molecular Property Counts

Molecular Property Counts are a simple and computationally efficient type of descriptor that represents the characteristics of a molecule based on the counts of different types of atoms and chemical bonds present. In this model, two Molecular Property Counts descriptors are involved: HBD_Count and Num_H_Donors_Lipinski. HBD_Count counts the number of groups that can act as hydrogen bond donors, while Num_H_Donors_Lipinski counts the number of heteroatoms (O, N, S, P) with hydrogen atoms. In this study, the structure of PI friction pair contains various hydrogen bond acceptors, such as oxygen atoms in carbonyl groups, nitrogen atoms in amine groups, and oxygen atoms in ether groups. These acceptors can form hydrogen bond interactions with hydrogen bond donors of the lubricant molecules, confirming the importance of hydrogen bonding in improving friction-reducing performance.

3.3.3. Solvent-Accessible Surface Area

Solvent Accessible Surface Area (SASA) is a geometric descriptor related to the three-dimensional conformation of a molecule. It describes the regions on the molecular surface that are accessible to solvent molecules and is calculated by simulating the positions and interactions of solvent molecules on the molecular surface. Among them, Molecular_PolarSASA refers to the polar solvent accessible surface area of the molecule. It is used to evaluate the size and distribution of polar regions in the molecule, providing information about the molecule's polarity characteristics. When calculating Molecular_PolarSASA, only atoms containing polar elements such as N, O, P, and S are selected to calculate their solvent accessible surface area, and their values are summed to obtain the final numerical value. This is because these elements typically exhibit strong interactions with solvents (such as water) and play an important role in the molecule's solubility and interactions.

Molecular_PolarSASA exhibits a strong negative correlation with the friction coefficient measurement in the model. This indicates that molecules with larger polar solvent accessible surface areas tend to have lower friction coefficients during the friction process, resulting in friction reduction. For example, in this sample set, glycerol has the largest

polar solvent accessible surface area, and its friction coefficient is close to the lowest value (COF = 0.004613), achieving a state of ultra-low friction.

3.3.4. Estate Keys

Estate Keys descriptors can be used to calculate numerical values related to the electronic topological state of specific atoms or record the count of specific types of atoms in a molecular structure. These descriptors are obtained by computing the molecular topology and electronic structure information, providing a comprehensive description of properties such as molecular topology, substituent groups, and electronegativity effects. In this model, a negatively correlated descriptor, ES_Count_sOH, is introduced, which represents the count of -OH groups present in the molecule. This indicates that the presence of hydroxyl or carboxyl groups in the molecule is beneficial for improving friction reduction.

3.3.5. AlogP

AlogP is an atom-based method used to calculate the octanol-water partition coefficient (LogP), which is an indicator of compound hydrophobicity (lipophilicity). It quantifies the tendency of a compound to partition between organic solvents and water. Higher AlogP values indicate greater lipophilicity, while lower AlogP values indicate greater hydrophilicity of the molecular. According to our model, AlogP values exhibit a positive correlation with the friction coefficient measurement. This suggests that organic lubricants with higher hydrophilicity may exhibit better friction-reducing performance in the friction system.

In the above discussion, we have explored in detail the impact of each descriptor on the friction-reducing performance of organic lubricants in the SiC/PI friction system. This provides valuable guidance for the initial screening of lubricant molecular structures. However, it is important to note that each descriptor is just one factor in lubricant design, and their influence on friction-reducing performance varies in terms of direction and weight. Considering the comprehensive impact of all descriptors and using the BPNN-QSTR model for quantitative calculations can provide a more accurate prediction and design of lubricant molecular structures with excellent friction-reducing performance. By taking into account multiple factors simultaneously, we can better understand the complex relationship between molecular descriptors and friction reduction, leading to more effective lubricant design and optimization.

4. Conclusions

In this study, the friction-reducing performance of 36 organic liquid compounds as lubricants in the SiC/PI friction pair was systematically tested. By using the backpropagation neural network method, a QSTR model was successfully established to predict the friction-reducing performance of these lubricants. The optimal network structure of the model was determined to be 11-5-1, with a result of R^2 = 0.9700, R^2 (*LOO*) = 0.6570, q^2 = 0.8606. The BPNN-QSTR model indicates that these five categories of descriptors, namely Jurs, Molecular Property Counts, Estate Keys, and the octanol-water partition coefficient, consisting of a total of 11 descriptors, influence the friction-reducing performance of the lubricants.

Compared to traditional qualitative analysis methods, quantitative analysis can comprehensively and accurately reveal the synergistic effects of molecular structural factors on lubricant friction reduction performance. The obtained model is characterized by simplicity, non-experimentality, and good predictive ability, making it suitable for screening or designing organic liquid lubricants with excellent friction-reducing performance. This is of great significance for the development of high-performance lubrication systems.

Author Contributions: Conceptualization, T.W., H.C., L.W. and X.G.; Data curation, L.Z.; Methodology, T.W., H.C., L.W. and X.G.; Software, L.W.; Validation, L.Z.; Writing—original draft, T.W.; Writing—review and editing, T.W. All authors have read and agreed to the published version of the manuscript.

Funding: This research was funded by Scientific research plan guidance project of Hubei Provincial Department of Education, grant number B2020060.

Data Availability Statement: Not applicable.

Conflicts of Interest: The authors declare no conflict of interest.

References

1. Stachowiak, G.W. How tribology has been helping us to advance and to survive? *Friction* **2017**, *5*, 233–247. [CrossRef]
2. Zhai, W.Z.; Zhou, K. Nanomaterials in superlubricity. *Adv. Funct. Mater.* **2019**, *29*, 1806395. [CrossRef]
3. Hirano, M.; Kazumasa, S. Atomistic locking and friction. *Phys. Rev. B* **1990**, *41*, 11837. [CrossRef] [PubMed]
4. Liu, Z.; Yang, J.R.; Grey, F.; Liu, Z.J.; Liu, Y.L.; Wang, Y.B.; Yang, Y.L.; Cheng, Y.; Zheng, Q.S. Observation of microscale superlubricity in graphite. *Phys. Rev. Lett.* **2012**, *108*, 205503. [CrossRef]
5. Zhang, B.; Ji, L.; Lu, Z.B.; Li, H.X.; Zhang, J.Y. Progress on engineering oriented solid superlubricity. *Tribology* **2023**, *43*, 3–17.
6. Ge, X.Y.; Li, J.J.; Luo, J.B. Macroscale superlubricity achieved with various liquid molecules: A review. *Front. Mech. Eng.* **2019**, *5*, 1–15. [CrossRef]
7. Han, T.Y.; Zhang, S.W.; Zhang, C.H. Unlocking the secrets behind liquid superlubricity: A state-of-the-art review on phenomena and mechanisms. *Friction* **2022**, *10*, 1137–1165. [CrossRef]
8. Kizilkaya, C.; Mülazim, Y.; Kahraman, M.V.; Apohan, N.; Güngör, A. Synthesis and characterization of polyimide/hexagonal boron nitride composite. *J. Appl. Polym. Sci.* **2012**, *124*, 706–712. [CrossRef]
9. Tian, J.; Wang, H.Y.; Huang, Z.Y.; Lu, R.G.; Cong, P.; Liu, X.J.; Li, T.S. Investigation on tribological properties of fluorinated polyimide. *J. Macromol. Sci. Part B* **2010**, *49*, 791–801. [CrossRef]
10. Min, C.Y.; Nie, P.; Song, H.J.; Zhang, Z.Z.; Zhao, K.L. Study of tribological properties of polyimide/graphene oxide nanocomposite films under seawater-lubricated condition. *Tribol. Int.* **2014**, *80*, 131–140. [CrossRef]
11. Zhang, D.; Wang, T.; Wang, Q.; Wang, C. Selectively enhanced oil retention of porous polyimide bearing materials by direct chemical modification. *J. Appl. Polym. Sci.* **2017**, *134*, 45106. [CrossRef]
12. Wang, C.; Zhang, D.; Wang, Q.; Ruan, H.; Wang, T. Effect of porosity on the friction properties of porous polyimide impregnated with poly-α-olefin in different lubrication regimes. *Tribol. Lett.* **2020**, *68*, 1–9. [CrossRef]
13. Ruan, H.; Shao, M.; Zhang, Y.; Wang, Q.; Wang, C.; Wang, T. Supramolecular oleogel-impregnated macroporous polyimide for high capacity of oil storage and recyclable smart lubrication. *ACS Appl. Mater. Interfaces* **2022**, *14*, 10936–10946. [CrossRef] [PubMed]
14. Buckley, D.H.; Miyoshi, K. Friction and wear of ceramics. *Wear* **1984**, *100*, 333–353. [CrossRef]
15. Boch, P.; Platon, F.; Kapelski, G. Tribological and interfacial phenomena in Al2O3/SiC and SiC/SiC couples at high temperature. *J. Eur. Ceram. Soc.* **1989**, *5*, 223–228. [CrossRef]
16. Cho, S.J.; Um, C.D.; Kim, S.S. Wear and wear transition mechanism in silicon carbide during sliding. *J. Am. Ceram. Soc.* **1995**, *78*, 1076–1078. [CrossRef]
17. Zhang, Z.H.; Nie, S.L.; Liao, W.J. Tribological behaviors of carbon fiber reinforced polyetheretherketone sliding against silicon carbide ceramic under seawater lubrication. *Proc. Inst. Mech. Eng. Part J J. Eng. Tribol.* **2014**, *228*, 1421–1432. [CrossRef]
18. Matsuda, M.; Kato, K.; Hashimoto, A. Friction and wear properties of silicon carbide in water from different sources. *Tribol. Lett.* **2011**, *43*, 33–41. [CrossRef]
19. Schreiber, P.J.; Schneider, J. Liquid superlubricity obtained for self-mated silicon carbide in nonaqueous low-viscosity fluid. *Tribol. Int.* **2019**, *134*, 7–14. [CrossRef]
20. Gao, X.L.; Wang, Z.; Dai, K.; Wang, T.T. A Quantitative structure tribo-ability relationship model for ester lubricant base oils. *J. Tribol.* **2015**, *137*, 021801. [CrossRef]
21. Gao, X.L.; Wang, T.T.; Cheng, Z. Quantitative structure tribo-ability relationship of ultra-high molecular weight polyethylene modified by inorganic compounds. *Ind. Lubr. Tribol.* **2018**, *70*, 182–190. [CrossRef]
22. Wang, T.T.; Wang, Z.; Chen, H.; Dai, K.; Gao, X.L. BPNN-QSTR models for triazine derivatives for lubricant additives. *J. Tribol.* **2020**, *142*, 011801. [CrossRef]
23. Li, B.R. *Structural Chemistry*; Higher Education Press: Beijing, China, 2011; pp. 638–664.
24. Bahadir, E. Prediction of prospective mathematics teachers' academic success in entering graduate education by using back-propagation neural network. *J. Educ. Train. Stud.* **2016**, *4*, 113–122. [CrossRef]
25. Gombar, G.V.K. The Importance of being earnest: Validation is the absolute essential for successful application and interpretation of QSPR Models. *QSAR Comb. Sci.* **2003**, *22*, 66–77.
26. Stanton, D.T.; Jurs, P.C. Development and use of charged partial surface area structural descriptors in computer-assisted quantitative structure-property relationship studies. *Anal. Chem.* **1990**, *62*, 2323–2329. [CrossRef]